

RESEARCH ARTICLE

Lionel G. Nowak · Jean Bullier

**Axons, but not cell bodies,
are activated by electrical stimulation in cortical gray matter****I. Evidence from chronaxie measurements**

Received: 25 January 1997 / Accepted 5 August 1997

Abstract Extracellular electrical stimulation of the gray matter is often used to determine the function of a given cortical area or pathway. However, when it is used to elicit postsynaptic effects, the presynaptic neuronal elements activated by electrical stimulation have never been clearly identified: it could be the excitable dendrites, the cell body, the axon initial segment, or the axonal branches. To identify these elements, we performed two series of experiments on slices of rat visual cortex maintained in vitro. The first series of experiments, reported in this paper, was aimed at determining the *chronaxie*, a temporal parameter related to the membrane properties of the neuronal elements. In order to identify the presynaptic elements that were activated by extracellular electrical stimulation, chronaxies corresponding to postsynaptic responses were measured and compared with those corresponding to the activation of axons (antidromic activation) and those corresponding to the activation of cell bodies (intracellular current injection in intracellularly recorded neurons). The chronaxie for orthodromic activation was similar to that for axonal activation, but was 40 times smaller than the chronaxie for direct cell body activation. This suggests that, whenever a postsynaptic response is elicited after electrical stimulation of the cortical gray matter, axons (either axonal branches or axon initial segments), but not cell bodies, are the neuronal elements activated.

Key words Visual cortex · Brain slice · Strength-duration relations · Conduction velocity · Rat

Introduction

Electrical stimulation of neuronal elements has been widely employed as a tool in the study of brain physiology for over a century. When axons are directly activated, the action potential can propagate back to the cell body and produce an antidromic activation, which has been used to study the physiology of neurons with identified targets (reviewed by Lipsky 1981; Swadlow 1983; for visual system, see also Henry et al. 1978; Harvey 1980).

The other applications of electrical stimulation all have in common the requirement that a postsynaptic target be activated. The induction of postsynaptic responses is used for different types of studies such as: the characterization of the synaptic potentials and the identification of the neurotransmitters and receptors involved in different types of connections; the study of the synaptic mechanisms responsible for the plasticity of the nervous system; the physiological properties and morphological features of neurons that are postsynaptic to other groups of neurons (Singer et al. 1975; Bullier and Henry 1979a–c, Deschênes et al. 1979; Martin and Whitteridge 1984; Kaneko et al. 1994); and the mapping of motor cortical areas (Asanuma and Sakata 1967; Andersen et al. 1975; Schiller et al. 1979; Cheney and Fetz 1985; Yeoman and Tehovnik 1988; Tehovnik and Lee 1993). Electrical stimulation applied within certain structures has also been used to induce or to modify a behavior (hypothalamus: Szabo and Milner 1972; Matthews 1977; neocortex: Komatsu and Wurtz 1989; Salzman et al. 1990; Tehovnik 1996). Finally, electrical stimulation has important potential clinical application, such as in the case of cochlear implants (Busby et al. 1992), in the development of cortical prosthesis for the blind (Brindley 1973; Dobbelle and Mladejovsky 1974; Bak et al. 1990), or the use of electrical stimulation to correct motor deficits associated with Parkinson disease (Caparros-Lefebvre et al. 1993).

Electrical stimulation acts by generating action potentials that are propagated from the site of stimulation along the axon. Action potential initiation occurs in the axon, but might also occur in the dendrite and the cell body

L.G. Nowak¹ · J. Bullier (✉)
INSERM Unité 371, "Cerveau et Vision," 18,
avenue du Doyen Lépine, F-69500 Bron, France

Present address:

¹ Section of Neurobiology, Yale University School of Medicine,
C303 Sterling Hall of Medicine, 333 Cedar Street,
New Haven, CT 06510, USA

(e.g., Stuart et al. 1997). The question that arises is: When a postsynaptic response is obtained after the stimulation of the gray matter, what are the presynaptic neuronal elements activated? The answer to that question is essential, because it will determine the interpretation of the results obtained. This is especially the case when stimulation is applied in structures such as the neocortex that receive multiple inputs both from local neurons and from structures with which the connections are usually reciprocal and where axons possess arborization both locally and at distance from the parent neuron.

The series of experiments reported in that paper was aimed at determining whether cell bodies or axons (either axonal branches or axon initial segments) are the presynaptic elements activated by extracellular electrical stimulation when it is used to produce a postsynaptic potential. The identification of the elements activated relied on their *temporal* properties, which were determined from the relationship between the duration and the threshold intensity of a current pulse inducing a given response (strength-duration relationship). We first established strength-duration curves for eliciting antidromic action potentials with extracellular stimulation (in which case the neuronal element activated was the axon). We then established strength-duration curves for eliciting action potentials with intracellular current injection in intracellularly recorded neurons (direct activation; the neuronal element activated was the cell body). Both were then compared with strength-duration curves established for eliciting an excitatory post-synaptic potential (EPSP) with extracellular stimulation in the gray matter (in which case the presynaptic element was unknown).

The results obtained with this first method suggest that axons, but not cell bodies, are the elements activated by electrical stimulation. In the second paper (Nowak and Bullier 1997), we report on experiments aimed at establishing what is the contribution of the different portions of the axon (axon initial segment or axonal branches) for the production of a postsynaptic response.

Materials and methods

Brain slice preparation

Recording and stimulation were performed in areas 17 and 18a of rat visual cortex maintained *in vitro*. Protocols for preparation and maintenance of brain slices have been described in details in another paper (Nowak and Bullier 1996) and are briefly presented here. The aorta of male or female Wistar or Sprague Dawley adult rats was cannulated under deep halothene anesthesia. The cannula was used to perfuse a modified artificial cerebrospinal fluid (mACSF) of the following composition: NaCl 91.7 mM; NaHCO₃ 24 mM; NaH₂PO₄ 1.2 mM; KCl 3 mM; MgCl₂ 19 mM; MgSO₄ 1 mM; and D-Glucose 25 mM. The mACSF was bubbled prior to perfusion with a mixture of 95% O₂ and 5% CO₂ and cooled to 3–4°C. During the perfusion the skull was drilled and the brain removed. Coronal slices (500 µm thickness) were cut with a vibratome (Oxford). Once obtained, slices were allowed to recover for at least 1 h in a medium containing a standard ACSF, which was also used for recording. Its composition was: NaCl 126 mM; NaHCO₃ 24 mM; NaH₂PO₄ 1.2 mM; KCl 3 mM; CaCl₂ 2.5 mM; MgSO₄ 1 mM; and D-glucose 10 mM. This

ACSF was continuously bubbled with a 95% O₂–5% CO₂ mixture (pH 7.4). For recording, one slice was transferred to a submersion-type chamber. The oxygenated ACSF was gravity fed at a flow rate of 6–8 ml/min and the temperature was maintained at 33–34°C.

Recording and stimulation

Intracellular recordings were made with glass micropipettes pulled on a BB-CH puller (Mecanex, Geneva) from 1.2-mm-OD capillaries (Clark Electromedical Instruments) and filled with 3 M of potassium acetate (d.c. resistance 80–120 MΩ). d.c. potentials were amplified by an amplifier (Biologic VF 180) containing an active bridge circuit as well as capacity and resistance compensations, followed by a Neurolog device containing amplifiers and filters. The intracellular recordings were filtered with a high-frequency cutoff of 1 kHz or 10 kHz (except when stated otherwise).

Extracellular recordings of single units were obtained with tungsten-in-glass microelectrodes (Merrill and Ainsworth 1972) with 15- to 25-µm exposed tips and plated with platinum black (impedance less than 0.5 MΩ at 1000 Hz). The Neurolog recording system was used for amplification and filtering. Filtering was adjusted for individual recordings to give a proper signal-to-noise ratio. Tungsten-in-glass microelectrodes plated with platinum black were also used for electrical stimulation. The glass was removed over a length of 15–25 µm. Electrical stimulation consisted of monopolar, cathodal pulses delivered at a frequency of 0.5 Hz or 0.3 Hz through a stimulation isolation unit (Neurolog).

Criteria for the identification of antidromic activation

Antidromic action potentials observed in intracellularly recorded neurons were identified by their constant latency and by the absence of an underlying EPSP. The presence of an initial segment spike that sometimes occurred without a somatodendritic spike further facilitated their identification.

When extracellularly recorded, antidromic action potentials were identified according to the following criteria: (a) no variation of latency with current having an intensity equal to 1.5 times the threshold current intensity; (b) less than 10% decrease in latency when current intensity was raised from threshold to twice the threshold; (c) a refractory period of less than 3 ms, (d) the ability to sustain high-frequency (100 Hz or more) stimulation for 200 ms. In well-isolated recordings, it was also possible to distinguish an inflection in the rising part of the action potential, corresponding to the presence of an I5 spike followed by the SD spike. The validity of these criteria for the identification of antidromic action potentials has been confirmed in five cases for which recordings were performed in a medium where Ca²⁺ was replaced by 2 mM of Mn²⁺.

The conduction velocity was determined by dividing the distance between stimulating and recording electrode (determined from the cursors of the micromanipulators) by the latency of antidromic activation (measured between the stimulus onset and the foot of the action potential).

Results

Recording and stimulation were performed in areas 17 and 18a of rat visual cortex. Some of the results presented in this paper were obtained from neurons involved in corticocortical connections between these two areas. The localization of the parts of areas 17 and 18a that are connected in brain slices and the characteristics of the field potentials elicited through corticocortical connections are described in another paper (Nowak et al. 1997).

Recordings were obtained either intracellularly or extracellularly. The 17 neurons intracellularly recorded for

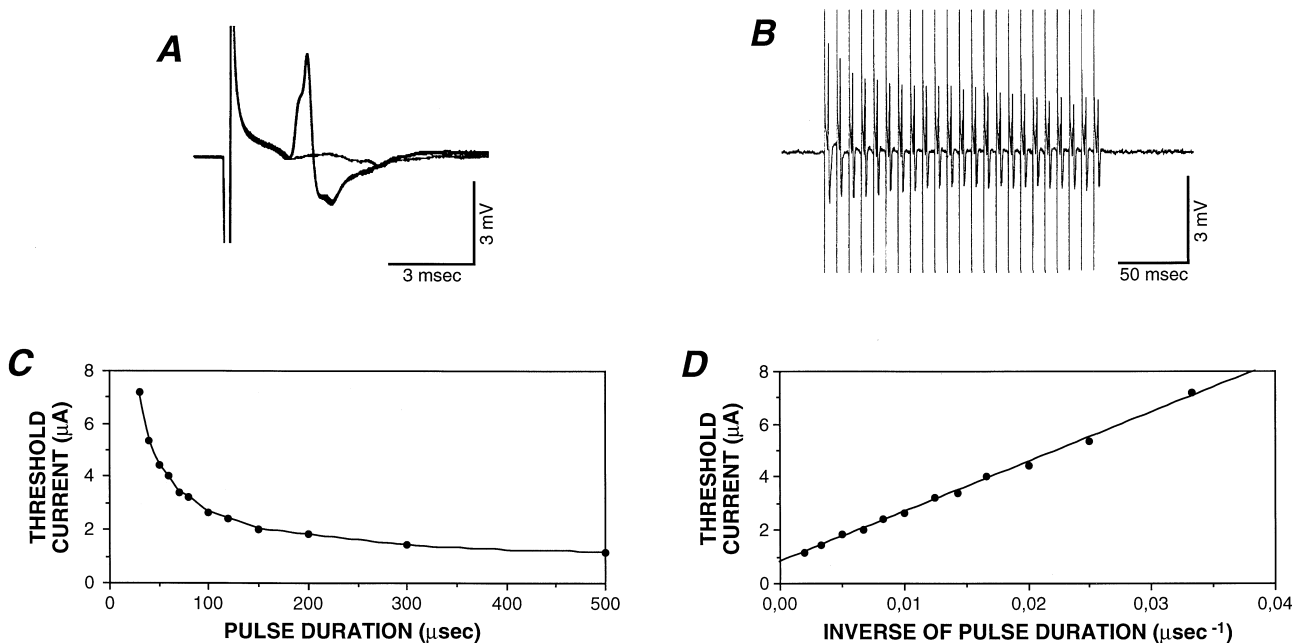


Fig. 1A–D Chronaxie for antidromic (axonal) activation. The cell was recorded in the supragranular layers of area 17 and the electrical stimulation was applied in layer 6 of area 17. **A** Activation of the cell with a threshold current intensity. **B** Response of the same cell to a high-frequency (115 Hz) train of pulses applied for 200 ms. **C** Plot of threshold current intensity (I , in microamperes) as a function of the duration (t , in microseconds) of the pulse used to evoke the antidromic action potential. **D** Plot of threshold current as a function of the inverse of the pulse duration. The relationship is clearly linear. The regression line is $I=187.84/t+0.80$ ($r^2=0.998$). The rheobase is $0.80 \mu\text{A}$. The slope (187.84) corresponds to the product of the rheobase times the chronaxie (C); $C=235 \mu\text{s}$. In this and the following figures, positive potential is upward

Chronaxie for antidromic activation

Figure 1 shows results obtained for an antidromically elicited action potential. The neuron was extracellularly recorded in the supragranular layers of area 17 and its axon was activated by electrical stimulation applied in layer 6 of the same area. Figure 1A shows four superimposed sweeps (three successes, one failure) obtained with a threshold current intensity. The rising part of the action potential is diphasic, a feature of some antidromic action potentials. When present, the action potential shows little, if any, latency jitter. Figure 1B shows that this neuron was able to follow a high-frequency stimulation (115 Hz) applied during 200 ms, which further confirms its antidromic nature.

The strength-duration curve for that cell is illustrated in Fig. 1C. The threshold corresponds here to the current intensity leading to the occurrence of an antidromic action potential in about 50% of the trials. The strength-duration curve shows that it is possible to compensate for decreases in current intensity by increasing the pulse duration. However, the relationship between the duration and the intensity of the stimulation pulse is not linear: as the duration is increased, the threshold current decreases toward an asymptotic value.

Two measures can be extracted from strength-duration curves, the rheobase and the chronaxie. The rheobase corresponds to the horizontal asymptote in the strength-duration curve. The chronaxie is classically defined as the *duration* of the threshold current pulse having an intensity twice that of the rheobase.

To accurately determine chronaxies, we plotted the threshold current against the inverse of the pulse duration. This is shown in Fig. 1D for the same cell. This curve can be fitted by a straight line, the equation of which is $I=I_0+I_0C/t$, in which I is the threshold current (in microamperes), I_0 is the rheobase (in microamperes), C the

that study were all located in the supragranular layers. The membrane properties of 15 of them (data about the remaining two cases were lost) were as follow (mean \pm SD): they had a resting membrane potential of -77.9 ± 8.8 mV; an input resistance (determined by current injection of -0.1 nA) of 31.9 ± 10.9 M Ω ; their time constant (determined from current injection of -0.1 nA as the time to reach 63% of the maximal hyperpolarization) was 6.1 ± 2.7 ms; they displayed overshooting action potentials, the amplitude of which was 104.9 ± 13.0 mV when measured from resting membrane potential or 77.7 ± 9.2 mV when measured from the spike threshold. These neurons presented accommodative discharge properties together with relatively wide action potentials (width measured at half the action potential height from threshold, 0.61 ± 0.11 ms), with a depolarization phase faster than the repolarization. These properties are characteristic of regular spiking neurons (Connors et al. 1982; McCormick et al. 1985).

The term “axon” used without further precision will designate both axonal branches (or axons “en passant”) and axon initial segment. The term “cell body” is to be understood as the cell body, *not* including the axon initial segment.

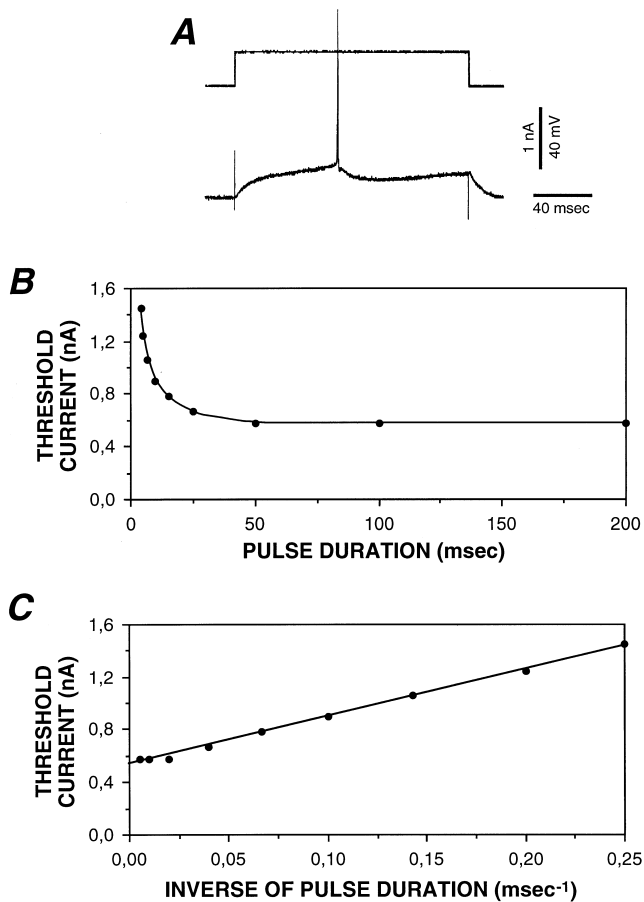


Fig. 2A–C Chronaxie for direct cell-body activation. The neuron was intracellularly recorded in the supragranular layers of area 18a. The response of the cell to a current injection larger than threshold appears in **A**. **B** Plot of the threshold intensity to elicit an action potential as a function of the duration (milliseconds) of the intracellularly injected current pulse. **C** Plot of threshold current compared with the inverse of the pulse duration. The regression line is $I=0.536+3.592/t$ ($r^2=0.997$). The chronaxie is 6.8 ms

chronaxie (in microseconds), and t the pulse duration (in microseconds). Values of I_0 and I_0C are given by the linear regression. Chronaxie can then be extracted. The chronaxie for the case illustrated in Fig. 1 was 235 μ s.

Chronaxie for intracellularly elicited action potentials

To determine the chronaxies corresponding to direct cell body activation, we established strength-duration curves for nine intracellularly recorded neurons. The stimulation current was injected *inside* the neurons through the recording micropipette. Contrary to extracellular stimulation, the micropipette was used as the anode. The effect to be produced was the occurrence of an action potential, with a 50% success criterion to define the threshold current. Figure 2 illustrates the results obtained for one neuron. The relationship between threshold intensity and pulse duration is presented in Fig. 2B and the linear relationship between the inverse of the pulse duration and the

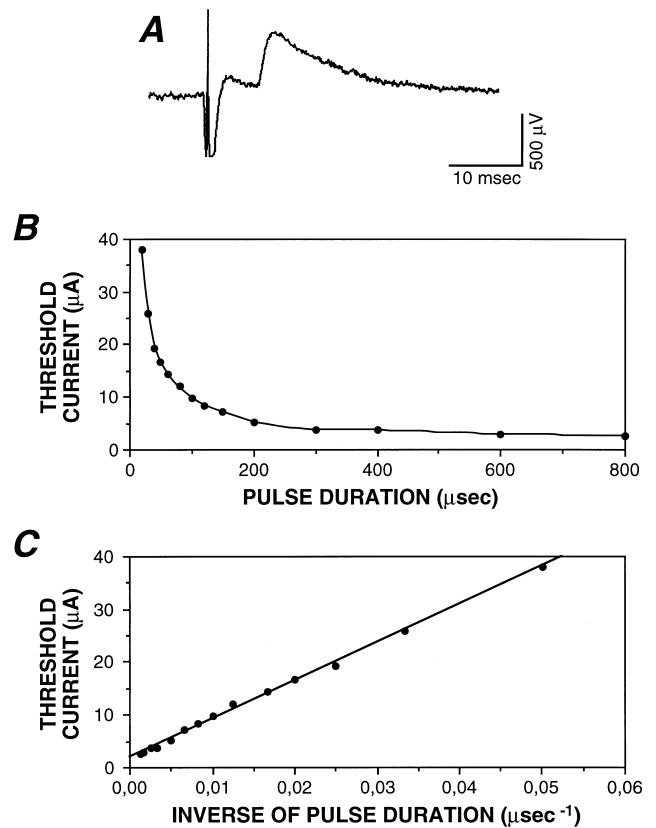


Fig. 3A–C Chronaxie for orthodromic activation. The cell was recorded in the supragranular layers of area 18a. The stimulation was applied in the supragranular layers of area 17 to elicit a unitary EPSP. In that case, the presynaptic element activated by the electrical stimulation was unknown. **A** Unitary EPSP as it appears after the averaging of 50 sweeps. **B** Relationship between electrical stimulation pulse duration and threshold intensity. **C** Relationship between the inverse of the pulse duration and the threshold intensity. The best fit equation is $I=724.4/t+1.99$. The chronaxie extracted from this equation is 363.9 μ s

threshold intensity in Fig. 2C. The chronaxie, extracted from the best-fitting equation, was 6.8 ms in that case. This is 29 times larger than the chronaxie for axonal activation of the cell illustrated in Fig. 1.

Chronaxie for orthodromic activation

Strength-duration curves for eliciting orthodromic activation with extracellularly applied electrical stimulation have been established for 14 orthodromic responses. In one case a strength-duration curve was established for an orthodromic action potential elicited through cortico-cortical connections. A second case corresponded to a large, all-or-nothing, polysynaptic potential that was obtained with electrical stimulation applied in the same area as the recorded neuron. In these two cases a population of presynaptic elements was activated.

The remaining 12 cases corresponded to unitary EPSPs, i.e., EPSPs that were produced after the activation

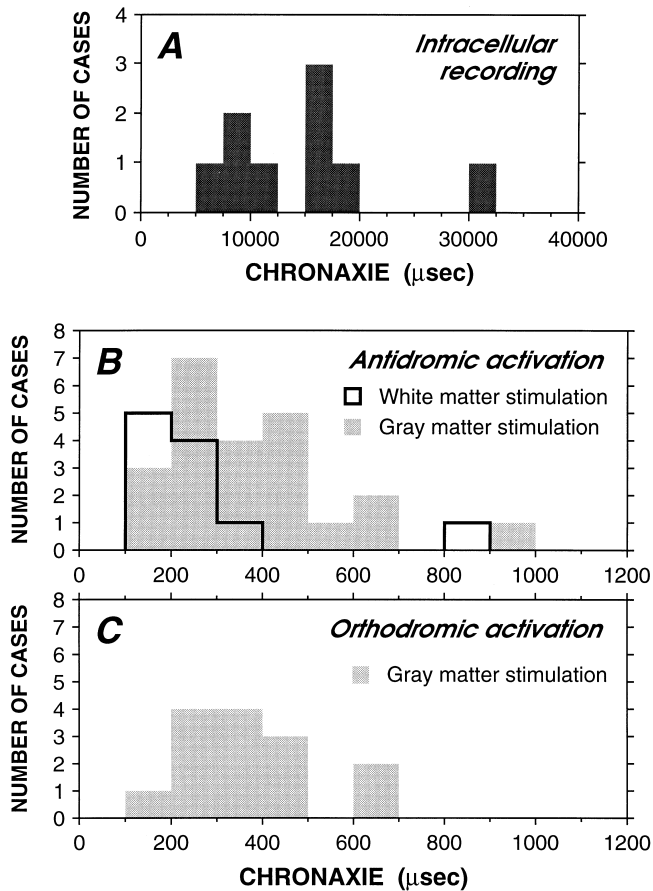


Fig. 4A–C Histograms for the distribution of chronaxies. **A** Distribution of chronaxies for the direct cell-body activation determined with intracellular current injection. **B** Distribution of chronaxies for antidromic activation. Recordings were intracellular for five neurons and extracellular for 29. The *thick-line histogram* corresponds to chronaxies obtained after stimulation in the white matter. Chronaxies obtained after stimulation in the gray matter appear in the *gray histogram*. **C** Histogram for chronaxies corresponding to orthodromic activation. All data obtained after stimulation in the gray matter

of a *single* presynaptic element. Their unitary nature was recognized by their small amplitude and their occurrence in an all-or-nothing fashion. The criteria to establish their monosynaptic nature was their short and constant latency, their fast rise time, and their ability to sustain high-frequency stimulation (up to 20 Hz). The mean amplitude

of the unitary EPSPs was 1.08 ± 0.27 mV. This corresponds to the upper range of unitary EPSPs observed in rat neocortex by spike-triggered averaging (Komatsu et al. 1988; Thomson et al. 1988), by dual intracellular recording (Mason et al. 1991; Nicoll and Blackmore 1993; Thomson and West 1993; Thomson et al. 1993), and are similar to those obtained by Volgushev et al. (1995) with a minimal electrical stimulation technique. Eight of the twelve unitary EPSPs were recorded in area 18a while electrical stimulation was applied in area 17. The remaining four unitary EPSPs were obtained with both stimulation and recording in area 17.

One example of a corticocortical unitary EPSP appears in Fig. 3A. The cell was recorded in the supragranular layer of area 18a while the stimulation was applied in the supragranular layer of area 17. The trace shown in Fig. 3A was obtained after the averaging of about 50 sweeps.

For the establishment of the strength-duration curves, the threshold current corresponded to the current leading to the occurrence of the EPSP in 50% of the trials. Therefore, it was necessary to determine in a single sweep whether the EPSP occurred or not. Owing to their small size however, the unitary EPSPs were difficult to extract from the noise in a single sweep. Therefore, the signal, unlike the case illustrated in Fig. 3A, was filtered. This filtering distorted the shape of the EPSP, but it could then be clearly seen in a single trial whether it occurred or failed to occur for a given stimulation intensity (the measurements of amplitude given above were made on unfiltered, averaged traces).

Figure 3B shows the relationship between the threshold current and the pulse duration for the EPSP shown in Fig. 3A. Figure 3C is the corresponding plot of the threshold current as a function of the inverse of the pulse duration. It is again well fitted by a line. For this particular case, the chronaxie was 363.9 μ s.

Comparison of chronaxies

Summary data on the chronaxies are given in Table 1 and Fig. 4. The upper histogram in Fig. 4A corresponds to chronaxies for *intracellularly elicited action potentials* with intracellular current injection. The mean value (\pm SD) was 15004 ± 7376 μ s.

Table 1 Chronaxie values (in microseconds)

	Number	Mean	SD	SEM	Minimum	Maximum	Median
Antidromic, white matter	11	271.5	204.7	61.7	106.2	834.7	203.9
Antidromic, gray matter							
All	23	379.6	191.2	39.9	176.6	971.1	344.5
Corticocortical	6	406.5	289.0	118.0	209.8	971.7	280.1
Intrinsic connections	17	370.1	154.3	37.4	176.6	658.3	354.3
Orthodromic, gray matter							
All	14	379.7	145.1	38.8	166.8	676.9	348.1
Corticocortical	9	430.1	149.3	49.8	285.3	676.9	363.9
Direct (intracellular)	9	15004	7376	2459	6825	31290	15467

It has been suggested on theoretical ground that chronaxie is related to the neuronal time constant, although not in a simple way (Ranck 1975; Bostock 1983; Jack et al. 1983). The time constant of the neurons for which intracellular chronaxies were established averaged 7.0 ± 2.5 ms, but it did not appear to be correlated to the chronaxie. Nevertheless, both measures are of the same order of magnitude.

The lower two histograms (Fig. 4B, C) correspond to case where extracellular electrical stimulation was used. Notice that the scale of these histograms is different from that of the upper one. Chronaxies corresponding to *antidromic activation*, and therefore to axonal stimulation, were determined for 34 neurons and their distribution appears in Fig. 4B. Electrical stimulation was applied in the white matter in 11 cases (*thick-line histogram* in Fig. 4B) and in the gray matter in 23 cases (gray histogram in Fig. 4B). The mean (\pm SD) chronaxie for stimulation applied in the white matter was 271.5 ± 204.7 μ s. The mean chronaxie for stimulation applied in the gray matter was 379.6 ± 191.2 μ s. Chronaxies obtained after stimulation of axons in the gray matter were significantly larger than those obtained after stimulation of axons in the white matter ($P=0.03$, Mann-Whitney U -test).

Electrical stimulation for antidromic activation in the cortical gray matter was applied either in the same area as the recorded neuron (intrinsic connections, $n=17$) or in another cortical area (corticocortical connections, $n=6$). Chronaxies for antidromic activation through corticocortical connections (mean 406.5 ± 289.0 μ s) were not significantly different from chronaxies obtained for intrinsic connections (370.1 ± 154.3 μ s; Mann-Whitney U -test, $P=0.89$).

The distribution of chronaxies obtained after *orthodromic activation* appears in Fig. 4C. In all the cases, the electrical stimulation was applied in the gray matter. The mean was 379.7 ± 145.1 μ s ($n=14$). For the sample of orthodromic activation obtained through corticocortical connections, the mean was 430.1 ± 149.3 μ s ($n=9$). Comparing the gray histograms of Fig. 4B and C shows that the distribution of chronaxies corresponding to orthodromic activation, for which the presynaptic neuronal element activated was unknown, is very similar to that corresponding to antidromic activation, in which case the neuronal element activated was the axon (Mann-Whitney U -test, $P=0.63$). If the comparison is restricted to the sample of corticocortical connections, the distributions of chronaxies for antidromic and orthodromic activation remain similar (Mann-Whitney U -test, $P=0.24$). Both distributions are very different from that corresponding to the direct activation of cell bodies (Fig. 4A). The chronaxies determined for direct cell-body activation are 40 time larger on average than those obtained with extracellular electrical stimulation in the gray matter, both for orthodromic and antidromic activation. These results suggest that, whenever an orthodromic activation is obtained after electrical stimulation in the cortical gray matter, the axon and not the cell body is the presynaptic element activated.

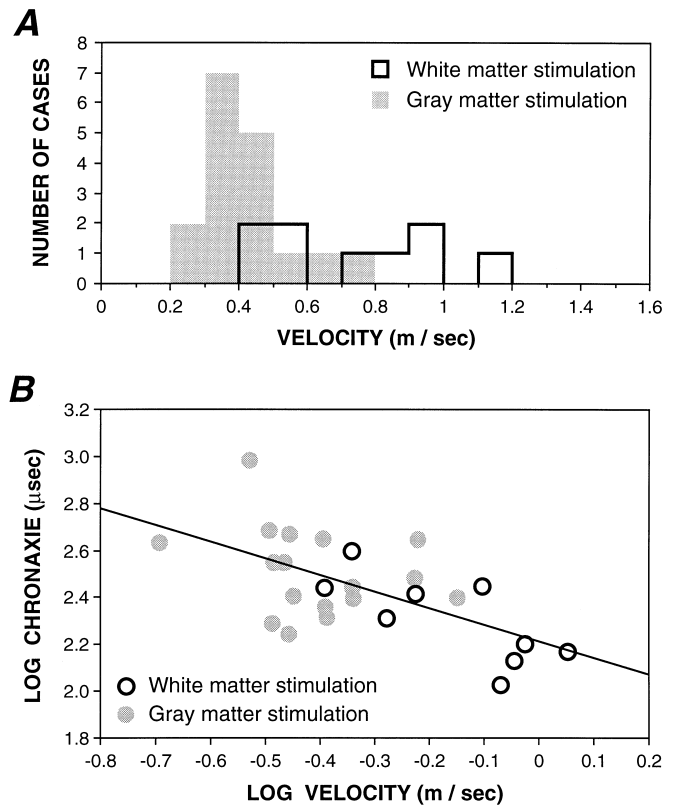


Fig. 5A, B Conduction velocity and chronaxie. **A** Distribution of axonal conduction velocities determined for antidromically activated neurons. *Gray bars histogram*, stimulation in the gray matter; *thick-line histogram*, stimulation in the white matter. The sample size is smaller than in Fig. 4B, because the distance between stimulating and recording electrode has not been determined in all the cases. **B** Relationship between the log of conduction velocity (v) and that of chronaxie (C) for antidromically activated neurons after stimulation in white (*empty black circles*) and gray (*filled gray circles*) matter. The best-fit equation is $\log(C) = -0.71 \log(v) + 2.212$ ($r^2 = 0.388$)

Chronaxie and conduction velocity

Figure 5A is a histogram of the conduction velocity of the neurons that were antidromically activated. The gray bars correspond to the cases for which electrical stimulation was applied in the gray matter. The thick-line histogram represents the conduction velocity of axons that were activated after stimulation of the white matter. The conduction velocity of axons activated from the white matter was higher than that of axons activated from the gray matter (Fig. 5A). The mean velocities were, respectively, 0.734 ± 0.249 m/s ($n=9$) and 0.405 ± 0.127 m/s ($n=17$). The difference proves to be highly significant (Mann-Whitney U -test, $P=0.0011$).

The relationship between chronaxie and conduction velocity (logarithmic values) is shown in Fig. 5B. The two parameters appear to be correlated ($r = -0.623$, $P = 0.007$). The neurons having the fastest conduction velocities are also those having the shortest chronaxies. This is particularly evident in the case of white matter stimulation.

Discussion

To identify the neuronal elements activated by electrical stimulation, we measured their chronaxies, which is a parameter related to their *temporal* properties. When electrical stimulation was applied in the cortical gray matter, the chronaxies corresponding to axonal activation (antidromic activation) were found to be very similar to those obtained when electrical stimulation was leading to orthodromic activation (mean 379.6 and 379.7 μ s, respectively). Both were very different from the chronaxies obtained with intracellular current injection in intracellularly recorded neurons that leads to direct cell-body activation (15004 μ s). This led us to conclude that, when a postsynaptic response is obtained after electrical stimulation in the cortical gray matter, it results from the activation of axons, rather than from that of cell bodies.

Methodology

Another measurement to identify the elements activated by electrical stimulation could have been the threshold for their activation. However, since data were obtained either with intracellular or with extracellular stimulation, it is impossible in our case to compare thresholds because: (1) the threshold increases as a function of the distance between the extracellular stimulating electrode tip and the element activated (Nowak and Bullier 1996); this distance could not be determined accurately given the impossibility to visualize axons or cell bodies in 500- μ m-thick slices. (2) The extracellular and intracellular medium resistivities, therefore the voltage gradients responsible for neuronal activation, are probably different; and (3) the electrode types used are likely to present very different current densities due to differences in surface (about 0.3 μ m² for intracellular electrodes, and the surface of a cone of approximately 700 μ m² for extracellular stimulating electrodes).

The conclusion we reached after chronaxie measurements – that cell bodies are not activated by extracellular electrical stimulation – is valid only if the two types of stimulation we used – extracellular stimulation applied through tungsten-in-glass microelectrodes at some distance from the neuronal elements, and intracellular stimulation applied through glass micropipettes used for recording of cell bodies – are comparable in terms of activation time course. In other words, it must be assumed that extracellular stimulation has the same effect as intracellular stimulation. Extracellular cathodal stimulation acts by removing positive charges from the extracellular space (Ranck 1981; Rattay 1987; Coburn 1989), while intracellular injection of current depolarizes cells by adding positive charges to the intracellular space. Calculations have been done showing that the withdrawal of current from outside a fiber is equivalent to the intracellular injection of current (Bostock 1983).

However, a first potential problem is that the thin and long shank of glass micropipettes used for intracellular re-

ording and stimulation may display a large capacity. This could have introduced an artifactually long chronaxie for the intracellularly elicited action potentials. To determine whether there was such a capacity effect, we measured the time course of the potential increase in ACSF without capacity and resistance compensation. Using a current intensity of 0.7 nA (the mean current corresponding to chronaxies for direct cell-body activation) and an electrode of 100 M Ω resistance, the time constant of the exponential potential increase was 690 μ s and the potential reached a stable value in 3.15 ms, that is, in a time roughly 5 times faster than the mean chronaxie determined for intracellularly elicited action potentials. This indicates that the capacity of the micropipettes was not responsible for these long chronaxies, which are therefore determined by the membrane properties of the cell body.

With extracellular stimulation, a second problem is related to the separation between the stimulating electrode and the activated element, which, according to both theoretical and experimental studies, can influence the shape of the strength-duration curves: The length over which an axon is depolarized is proportional to the square root of the distance between the stimulating electrode and the activated element (Rattay 1987); it is also known that the time course of the depolarization is longer when the area of depolarized membrane increases (Jack et al. 1983). Therefore, the chronaxies must be shorter when the distance decreases. This has been shown theoretically and experimentally (Jack et al. 1983; West and Wolstencroft 1983; Reilly et al. 1985; Reilly and Bauer 1987). It follows that the chronaxie values we report here for extracellular stimulation would have been even smaller if the electrode was touching the stimulation axon. This, however, would have *strengthened* the already very large difference we report between the chronaxies determined for the activation of intracellularly recorded neurons and those obtained with extracellular stimulation.

That intracellular and extracellular electrical stimulation gives similar chronaxie is strongly supported by some experimental data: Franck and Fuortes (1956) and Hunt and Kuno (1959) determined strength-duration relations for *axons* that were *intracellularly* recorded in the spinal cord, by injecting intracellular depolarizing current pulses. In both studies, the chronaxies obtained were of about 200 μ s. This is similar, although larger, to the chronaxies established for the same types of axons with *extracellular* stimulation (50–200 μ s: Bement and Ranck 1969; Jankowska and Roberts 1972; Tkacs and Wurster 1991). As far as axons are concerned, chronaxies determined with extracellular stimulation are clearly very close to those determined with intracellular stimulation.

Fitting strength-duration curves

The equation we used for the fitting of the strength-duration relationship is, expressed in another way, the equation established by Weiss (1901), $It=I_0(C+t)$. This expression shows that the charge required for the activation of a

neuronal element is *not* a constant, but instead varies as a function of the pulse duration. This equation gave a better fit than the more-often-used equation of Lapicque (1907), $I=I_0/[1-\exp(-t/\tau_{SD})]$, τ_{SD} being the strength-duration time constant. After linearization, and when $I=2I_0$, the chronaxie can be calculated as $C=0.69 \tau_{SD}$. After linearization however, the quality of the fit depends strongly on the threshold current determined for long-duration pulses, which are the most difficult to determine accurately. On the contrary, the formula of Weiss, as we used it, placed emphasis on the thresholds determined for short-duration pulses, the easiest to determine with precision. The correlation coefficients we obtained with this formula were always larger than 0.98.

In addition, Bostock (1983) showed that, on theoretical grounds, fitting strength-duration curves with Lapicque's formula can lead to erroneous estimates of chronaxies. In that respect, we found that the strength-duration curves established using the linear transform of Lapicque's formula were often parabolic rather than linear. Therefore, both pragmatic and theoretical considerations suggest that the fitting of strength-duration curves and the values of chronaxie it yields are more accurate with Weiss's formula.

Comparison with other studies and relationship with conduction velocity

The chronaxie values we report for axonal (antidromic) activation in the gray matter range from 176 to 971 μ s, while electrical stimulation in the white matter yielded chronaxie values ranging from 106.2 to 834.7 μ s. Slightly shorter chronaxies (about 240 μ s) have been obtained after stimulation in the cortical gray matter of awake monkey area 17 (DeYoe et al. 1989). Asanuma et al. (1976) reported even smaller values (60–130 μ s) for the activation of intrinsic collaterals of pyramidal tract cells in the cat motor cortex. When stimulated in the spinal cord gray matter, motor cortex cell axons yielded a mean chronaxie of 110 μ s (Shinoda et al. 1976). It should be mentioned that motor cortex axons have a much higher conduction velocity (in excess of 5 m/s up to 76 m/s; Phillips 1956; Takahashi 1965; Koike et al. 1968, 1970; Deschênes et al. 1979) than those of rat visual cortex.

Chronaxies have been determined for subcortical structures and appear to vary widely depending on the structure stimulated, between 50 μ s and more than 1 ms (see Ranck 1975 for review; more recent data in Li and Bak 1976; Matthews 1978; Bostock et al. 1983; Hentall et al. 1984; van der Honert and Stypulkowski 1984; Morrison and Gebber 1985; Grant and Highfield 1991; Shizgal et al. 1991; Tkacs and Wurster 1991).

In a number of the studies mentioned above, it has been shown that chronaxie is shorter for fast-conducting axons. Therefore, the long chronaxie values we obtained may be linked to the slow conduction velocity of axons of rat visual cortex. The conduction velocities we report (0.405 m/s for gray matter stimulation, 0.734 m/s for

white matter stimulation on average) are within the range of conduction velocities reported for the axons of rodent and lagomorph visual cortex (Swadlow 1974; Swadlow and Weyand 1981; Lohmann and Rörig 1994). The conduction velocity of axons activated from the white matter was higher than that of axons activated from the gray matter. A possible explanation for this difference is that stimulation in the gray matter activated mainly thin-diameter, slowly conducting axon collaterals rather than the main axonal trunk. Alternatively, different levels of myelination could account for this difference. This suggests that there could be two types of neurons, characterized by different conduction velocities. Those having axons traveling in the white matter (callosal neurons for example), and those having axons traveling in the gray matter (neurons involved in ipsilateral corticocortical connections of the rodent for example).

We found an inverse relationship between conduction velocity and chronaxie (Fig. 5B). A similar relationship between these two parameters has also been obtained by Swadlow (1992). This indicates that some of the parameters that influence chronaxie may also influence conduction velocity. Axonal diameter and myelination could be some of these. The relationship between conduction velocity and chronaxie may also be related to differences in passive and active membrane properties for slow- and fast-conducting axons.

Activation of cell bodies and axons

The chronaxie measured by Koike et al. (1970) in cat motor cortex with *intracellular* current injection was an average 9.8 ms for fast, and 27.1 ms for slow pyramidal tract cells. These values are similar to those we report for chronaxies of cell bodies obtained with intracellular current injection (range 6.8–31.3 ms).

Several authors have established strength-duration relations with *extracellular* stimulation applied in the close vicinity of cell bodies. However, the chronaxies they obtained, in what was initially supposed to be a direct cell-body activation, are about 2 orders of magnitude smaller than those determined with intracellular stimulation of cell bodies: Values between 100 and 400 μ s have been reported (Stoney et al. 1968; Asanuma et al. 1976; Hentall et al. 1984; Kang et al. 1988; Swadlow 1992), which are comparable with the chronaxie values obtained for axonal activation.

Gustafsson and Jankowska (1976) applied extracellular electrical stimulation in the vicinity of spinal motoneurons that were intracellularly recorded. Under these conditions, they observed that the action potentials elicited in motoneurons were *always* preceded by an initial segment spike, even when the stimulating electrode was located far away in the dendritic field. This points to the fact that, when juxtosomal extracellular stimulation is used, it is the axon that is activated first, not the cell body itself. On the basis of less direct evidence, Swadlow (1992) reached the same conclusion. Therefore, the

chronaxies that have been reported for juxtosomal stimulation are likely to reflect not the direct activation of the cell body but that of the axon leaving it.

It has been shown that not only antidromic activation potentials but also orthodromic action potentials and action potentials elicited by intracellular current injection, are first initiated in the axon (in the initial segment or in the first node of Ranvier) before invading the cell body and the dendrites (for review, Stuart et al. 1997; see also Colbert and Johnston 1996). This indicates that the threshold for action potential initiation is lowest in the axon. The strength-duration curves indicate that there are two possible reasons why the threshold for action potential initiation can be lowest in the axon compared with the cell body. One is related to the time it takes to reach threshold, the order to the "absolute threshold" (the rheobasic current, independent from neuronal temporal properties).

Sodium channel density and threshold for cell body and axon activation

Although, for the reasons given above, we could not compare the threshold for activation between cell bodies and axons, direct electrophysiological evidence that the threshold current with *intracellularly* injected depolarizing pulses is lower for axons than for cell bodies has been given by Franck and Fuortes (1956), who found that the rheobasic current for the activation of motoneuron cell bodies is higher (mean 7.4 nA) than that required to activate intracellularly recorded axons (1.7 nA). Modeling studies have shown that the rheobasic current decreases as the sodium channel density increases (Bostock 1983). If the sodium channel density is different at the level of cell bodies and dendrites compared with axons, it may provide one explanation why the activation of the latter is favored by extracellular electrical stimulation.

Data from the literature indicates that the sodium channel density is much lower on somatodendritic membrane than on axonal membrane. For vertebrate unmyelinated axons, this density is around 100–200 channels/ μm^2 (Ritchie et al. 1976; Pellegrino et al. 1984). At the level of the node of Ranvier of myelinated axons, however, the sodium channel density can be much higher (12000 channels/ μm^2 ; Ritchie and Rogart 1977). The absolute sodium channel density on cell bodies (and dendrites) of neocortical neurons has not been established by labeling studies, but it can be extrapolated knowing the sodium conductances of pyramidal neuron cell bodies (60–100 pS/ μm^2 in Huguenard et al. 1988; 40 pS/ μm^2 in Stuart and Sakmann 1994) and the conductance of single sodium channel (16 pS in Alzheimer et al. 1993). The density of sodium channels on the membrane of neocortical cell bodies and dendrites would be 2.5–7. The recent study of Colbert and Johnston (1996) also suggest a density of 3 or 4 channels/ μm^2 . It is possible, however, that all the channels in a patch are not active at the same time. A more conservative estimation would be of the order of

10 sodium channels/ μm^2 . This density is still 1 order of magnitude lower than that of unmyelinated axons, and about 2 orders of magnitude smaller than that of the node of Ranvier.

This difference in sodium channel density is confirmed by a number of labeling studies in which a direct comparison of sodium channel densities on axonal and somatic membrane has been made for the same type of neuron. In cell culture, it has been found that the sodium channel density is larger by a factor of 5–15 on the axon compared with the cell body (Catterall 1981; Boudier et al. 1985; Angelides et al. 1988; see also Westenbroek et al. (1989) for data on adult rat brain).

Time constant and capacitance of cell bodies and axons

The second reason why action potential initiation can be lowest in the axon compared with the cell body is related to possible differences in terms of temporal properties. The tradition in electrical stimulation is to use a pulse duration of 0.2 ms, more rarely of 0.5 ms. The question is whether, during this duration, the membrane potential will be brought to threshold equally well in axons and cell bodies. This is determined for a large part by the membrane time constant (τ_m), which corresponds to the product of the specific membrane resistivity (R_m) by the specific membrane capacitance (C_m).¹

The R_m of unmyelinated axons is between 1000 and 5000 $\Omega\cdot\text{cm}^2$ (Hill 1984) and would be between 25 $\Omega\cdot\text{cm}^2$ and 125 $\Omega\cdot\text{cm}^2$ at the node of Ranvier (Hill 1984; Blight 1985). For cell bodies, recent whole-cell patch-clamp studies gave R_m values ranging between 20,000 and 200,000 $\Omega\cdot\text{cm}^2$ (Spruston and Johnston 1992; Major et al. 1994; Larkman et al. 1994). Therefore, the specific membrane resistivity appears to be higher for cell bodies than for axons. If we assume that C_m is similar for axons and cell bodies, the time constant for neuronal cell bodies should be longer than that for unmyelinated axons by a factor of 4 to 200, and longer than that for myelinated axons by a factor of 160 to 8000. In other words, for a given intensity of stimulation, the axons are likely to be depolarized much faster than the cell bodies, and the threshold for action potential generation should be reached earlier in axons than in cell bodies.

Another factor that influences the excitability of cell bodies and axons is their capacitance, itself determined by their surface. The model of auditory axons of Colombo

¹ Using intracellular recording, we did not observe any correlation between the chronaxie and the time constant, although both values were of the same order of magnitude. This presumably results from the fact that the small hyperpolarizing current pulses we used did not only reveal the passive membrane time constant, but also the time course of the activation and inactivation of different voltage-dependent conductances. However, in their theoretical studies on axons, Bostock (1983) and Reilly and Bauer (1987) concluded that chronaxie is mainly determined by τ_m . Similarly, in our own modeling study (unpublished), we found a relationship between time constant and chronaxie, although both parameters are not linearly related.

and Parkins (1987) gives indication about the influence of the surface area of a neuronal element on its excitability with extracellular stimulation. They modeled a myelinated axon at the end of which was placed an unmyelinated terminal portion. This is similar to the situation of a cell body lying at the end of a myelinated axon. They found that increasing the length of the unmyelinated portion increases the chronaxie and decreases the excitability, up to a point where the stimulating current activates, not the unmyelinated terminal portion itself, but the first node of Ranvier some distance away. They concluded that the unmyelinated terminal portion, "because of its capacitance, could act as a current sink affecting the chronaxie". Applying the same reasoning to neocortex, it seems quite likely that the large capacitance imposed by the large surface of the cell body and adjoining dendrites makes it a poor candidate for a direct activation by extracellular stimulation.

If action potentials are first initiated in the axon, why are chronaxies obtained with intracellular stimulation so different from those obtained with extracellular stimulation? In the first case, the membrane potential reaches spike threshold at the level of the initial segment (or the first node of Ranvier) with a time course imposed by the temporal properties of the cell body and dendrites. On the other hand, when extracellular electrical stimulation is used, the time course of the membrane potential in the axon is less likely to be affected by the large capacitance of the cell body, due to the relative electrical isolation of the two compartments (see Mainen et al. 1995). This would explain why chronaxies are so different for intracellular and extracellular stimulation near cell bodies.

Conclusion

Our data and those from others all lead to the same conclusion: When extracellular electrical stimulation is applied in the gray matter, axons (either axonal branches or axon initial segments), but not cell bodies, are activated. Gustafsson and Jankowska (1976) concluded that, in the spinal cord, "the effect of extracellular stimuli are exerted primarily via spread of current to the initial segment of the axon and its depolarization." On the basis of strength-distance relationship, a similar conclusion was also obtained for hypoglossal neurons by Porter (1963), who stated that the "effects produced by threshold currents may be attributed to stimulation of nerve fibers rather than cell bodies adjacent to the cathode." Our results indicate that the same apply for neocortical neurons.

In the companion paper (Nowak and Bullier 1997), we examine the relative contribution of axonal branches and initial segments to the pool of presynaptic elements activated by extracellular electrical stimulation.

Acknowledgements We thank Pascale Giroud and Naura Chounlamountri for help during the experiments, Pierre-Marie Chorrier for help with the mechanics, Christian Urquizar for help with the

electronics. Thanks to G.E. Loeb for bibliographical references. Thanks to visitors at the Neuroscience meeting (Washington 1993), to M. Abeles, H.A. Swadlow, W.T. Newsome, and E.J. Tehovnik for their comments and criticisms on this work while it was in progress. This work was supported by H.F.S.P. RG 55/94. L.G.N. was supported by a fellowship from the Ministère de la Recherche et de la Technologie and by a fellowship from the Fyssen fondation.

References

- Alzheimer C, Schwindt PC, Crill WE (1993) Modal gating of Na⁺ channels as a mechanism of persistent Na⁺ current in pyramidal neurons from rat and cat sensorimotor cortex. *J Neurosci* 13:660–673
- Andersen P, Hagan PJ, Phillips CG, Powell TPS (1975) Mapping by microstimulation of overlapping projections from area 4 to motor units of the baboon hands. *Proc R Soc Lond [Biol]* 188:31–60
- Angelides K, Elmer LW, Loftus D, Elson E (1988) Distribution and lateral mobility of voltage dependent sodium channels in neurons. *J Cell Biol* 106:1911–1925
- Asanuma H, Sakata H (1967) Functional organization of a cortical efferent system examined with focal depth stimulation in cats. *J Neurophysiol* 30:35–54
- Asanuma H, Arnold A, Zarzecki P (1976) Further study on excitation of pyramidal tract cells by intracortical microstimulation. *Exp Brain Res* 26:443–461
- Bak M, Girvin JP, Hambrecht FT, Kufka CV, Loeb GE, Schmidt EM (1990) Visual sensation produced by intracortical microstimulation of the human occipital cortex. *Med Biol Eng Comput* 28:257–259
- Bement SL, Ranck JB (1969) A quantitative study of electrical stimulation of central myelinated fibers. *Exp Neurol* 24:147–170
- Blight AR (1985) Computer simulation of action potentials and afterpotentials in mammalian myelinated axons, the case for a lower resistance myelin sheath. *Neuroscience* 15:13–31
- Bostock H (1983) The strength-duration relationship for excitation of myelinated nerves: computed dependence on membrane properties. *J Physiol (Lond)* 341:59–74
- Bostock H, Sears TA, Sherratt RM (1983) The spatial distribution of excitability and membrane current in normal and demyelinated mammalian nerve fibres. *J Physiol (Lond)* 341:41–58
- Boudier JA, Berwald-Netter Y, Dellmann HD, Boudier JL, Couraud F, Koulakff A, Cau P (1985) Ultrastructural visualization of Na⁺-channels associated [125](alpha)-scorpion toxin binding sites on fetal mouse nerve cells in culture. *Brain Res Dev Brain Res* 20:137–142
- Brindley GS (1973) Sensory effects of electrical stimulation of the visual and paraviscual cortex in man. In: Autrum H, Jung R, Loewenstein WR, MacKay DM, Teuber HL (eds) *Central processing of visual information*. (Handbook of sensory physiology, vol VII/3, part B). Springer, Berlin Heidelberg New York, pp 583–594
- Bullier J, Henry GH (1979a) Ordinal position of neurons in cat striate cortex. *J Neurophysiol* 42:1251–1263
- Bullier J, Henry GH (1979b) Neural path taken by afferent streams in striate cortex of the cat. *J Neurophysiol* 42:1264–1270
- Bullier J, Henry GH (1979c) Laminar distribution of first-order neurons and afferent terminals in cat striate cortex. *J Neurophysiol* 42:1271–1281
- Busby PA, Tong YC, Clark GM (1992) Psychophysical studies using a multiple-electrode cochlear implant in patients who were deafened early in life. *Audiology* 31:95–111
- Caparros-Lefebvre D, Blond D, Vermersch P, Pecheux N, Guieu JD, Petit H (1993) Chronic thalamic-stimulation improves tremor and levodopa induced dyskinesias in parkinson disease. *J Neurol Neurosurg Psychiatry* 56:268–273
- Catterall WA (1981) Localization of sodium channels in cultured neural cells. *J Neurosci* 1:777–783

- Cheney PD, Fetz EE (1985) Comparable patterns of muscle facilitation evoked by individual corticomotoneuronal (CM) cells and by single intracortical microstimuli in primates: evidence for functional groups of CM cells. *J Neurophysiol* 53:786–804
- Coburn B (1989) Neural modeling in electrical stimulation. *CRT Crit Rev Biomed Eng* 17:133–178
- Colbert CM, Johnston D (1996) Axonal action-potential initiation and Na⁺ channel density in the soma and axon initial segment of subicular pyramidal neurons. *J Neurosci* 16:6676–6686
- Colombo J, Parkins CW (1987) A model of electrical excitation of the mammalian auditory-nerve neuron. *Hear Res* 31:287–312
- Connors BW, Gutnick MJ, Prince DA (1982) Electrophysiological properties of neocortical neurons in vitro. *J Neurophysiol* 48:1302–1320
- Deschênes M, Labelle A, Landry P (1979) Morphological characterization of slow and fast pyramidal tract cells in the cat. *Brain Res* 178:251–274
- DeYoe EA, Lewine J, Doty RW (1989) Optimal stimuli for the detection of intracortical currents applied to striate cortex of awake macaque monkeys. *Proc Ann Int Conf IEEE Eng Med Biol Soc* 11:934–936
- Dobelle WH, Mladejovsky MG (1974) Artificial vision for the blind: electrical stimulation of visual cortex offers hope for a functional prosthesis. *Science* 183:440–444
- Frank K, Fuortes MGF (1956) Stimulation of spinal motoneurons with intracellular electrodes. *J Physiol (Lond)* 134:451–470
- Grant SJ, Highfield DA (1991) Extracellular characteristics of putative cholinergic neurons in the rat laterodorsal tegmental nucleus. *Brain Res* 559:64–74
- Gustafsson B, Jankowska E (1976) Direct and indirect activation of nerve cells by electrical pulses applied extracellularly. *J Physiol (Lond)* 258:33–61
- Harvey AR (1980) A physiological analysis of subcortical and commissural projection of areas 17 and 18 of the cat. *J Physiol (Lond)* 302:507–535
- Henry GH, Lund JS, Harvey AR (1978) Cells of the striate cortex projecting to the clare bishop area of the cat. *Brain Res* 151:154–158
- Hentall ID, Zorman G, Kansky S, Field HL (1984) An estimate of the minimum number of brain stem neurons required for inhibition of a flexion reflex. *J Neurophysiol* 51:978–985
- Hill B (1984) Ionic channels of excitable membranes. Sinauer, Sunderland
- Honert C van der, Stypulkowski PH (1984) Physiological properties of the electrically stimulated auditory nerve. II. Single fiber recording. *Hear Res* 14:225–243
- Huguenard JR, Hamill OP, Prince DA (1988) Developmental changes in Na⁺ conductances in rat neocortical neurons: appearance of a slowly inactivating component. *J Neurophysiol* 59:778–795
- Hunt CC, Kuno M (1959) Properties of spinal interneurons. *J Physiol (Lond)* 147:346–363
- Jack JJB, Noble D, Tsien RW (1983) *Electrical current flow in excitable cells*. Oxford University Press, Oxford
- Jankowska E, Roberts WJ (1972) An electrophysiological demonstration of the axonal projections of single spinal interneurons in the cat. *J Physiol (Lond)* 222:597–622
- Kaneko T, Caria MA, Asanuma H (1994) Information processing within the motor cortex. I. Responses of morphologically identified motor cortical cells to stimulation of the somatosensory cortex. *J Comp Neurol* 345:161–171
- Kang Y, Endo K, Araki T (1988) Excitatory synaptic actions between pairs of neighboring pyramidal tract cells in the motor cortex. *J Neurophysiol* 59:636–647
- Koike H, Okada Y, Oshima T, Takahashi K (1968) Accomodative behavior of cat pyramidal tract cells investigated with intracellular injection of currents. *Exp Brain Res* 5:173–188
- Koike H, Mano N, Okada Y, Oshima T (1970) Repetitive impulses generated in fast and slow pyramidal tract cells by intracellularly applied current steps. *Exp Brain Res* 11:263–281
- Komatsu H, Wurtz RH (1989) Modulation of pursuit eye movements by stimulation of cortical areas MT and MST. *J Neurophysiol* 62:31–47
- Komatsu Y, Nakajima S, Toyama K, Fetz EE (1988) Intracortical connectivity revealed by spike-triggered averaging in slice preparations of cat visual cortex. *Brain Res* 442:359–362
- Lapicque L (1907) Recherches quantitatives sur l'excitation électrique des nerfs traitée comme une polarisation. *J Physiol (Paris)* 9:622–635
- Larkman AU, Major G, Stratford KJ, Jack JJB (1994) Dendritic geometry of pyramidal neurones in the visual cortex of the rat. In: Albowitz B, Albus K, Kuhnt U, Northdurft H-Ch, Wahle P (eds) *Structural and functional organization of the neocortex*. Springer, Berlin Heidelberg New York, pp 118–131
- Li CL, Bak A (1976) Excitability characteristics of the A- and C-fibers in a peripheral nerve. *Exp Neurol* 50:67–79
- Lipski J (1981) Antidromic activation of neurones as an analytic tool in the study of the central nervous system. *J Neurosci Methods* 4:1–32
- Lohmann H, Rörig B (1994) Long-range horizontal connections between supragranular pyramidal cells in the extrastriate visual cortex of the rat. *J Comp Neurol* 344:543–558
- Mainen ZF, Georges J, Huguenard JR, Sejnowski TJ (1995) A model of spike initiation in neocortical pyramidal neurons. *Neuron* 15:1427–1439
- Major G, Larkman AU, Jonas B, Sakmann B, Jack JJB (1994) Detailed passive cable models of whole-cell recorded CA3 pyramidal neurons in rat hippocampal slices. *J Neurosci* 14:4613–4638
- Martin KAC, Whitteridge D (1984) Form, function and intracortical projections of spiny neurons in the striate visual cortex of the cat. *J Physiol (Lond)* 353:463–504
- Mason A, Nicoll A, Stratford K (1991) Synaptic transmission between individual pyramidal neurons of the rat visual cortex in vitro. *J Neurosci* 11:72–84
- Matthews G (1977) Neural substrate for brain stimulation reward in the rat: cathodal and anodal strength-duration properties. *J Comp Physiol Psychol* 91:858–874
- Matthews G (1978) Strength-duration properties of single units driven by electrical stimulation of the lateral hypothalamus in rats. *Brain Res Bull* 3:171–174
- McCormick DA, Connors BW, Lighthall JW, Prince DA (1985) Comparative electrophysiology of pyramidal and sparsely spiny stellate neurons of the neocortex. *J Neurophysiol* 54:782–806
- Merrill EG, Ainsworth A (1972) Glass-coated platinum-plated tungsten microelectrodes. *Med Biol Eng* 10:662–672
- Morrison SF, Gebber GL (1985) Axonal branching patterns and funicular trajectories of raphespinal sympathoinhibitory neurons. *J Neurophysiol* 53:759–772
- Nicoll A, Blackmore C (1993) Single-fiber EPSPs in layer 5 of rat visual cortex in vitro. *Neuroreport* 4:167–170
- Nowak LG, Bullier J (1996) Spread of stimulating current in the cortical grey matter of rat visual cortex studied on a new in vitro slice preparation. *J Neurosci Methods* 67:237–248
- Nowak LG, Bullier J (1997) Axons, but not cell bodies, are activated by electrical stimulation in cortical grey matter. II. Evidence from selective inactivation of cell bodies and axon initial segments. *Exp Brain Res* 118:489–500
- Nowak LG, James AC, Bullier J (1997) Corticocortical connections between visual areas 17 and 18a of the rat studied in vitro: spatial and temporal organization of functional synaptic responses. *Exp Brain Res* 117:219–241
- Pellegrino RG, Spencer PS, Ritchie JM (1984) Sodium channels in the axolemma of unmyelinated axons: a new estimate. *Brain Res* 305:357–360
- Phillips CG (1956) Intracellular records from Betz cells in the cat. *Q J Exp Physiol* 41:58–69
- Porter R (1963) Focal stimulation of hypoglossal neurones in the cat. *J Physiol (Lond)* 169:630–640
- Ranck JB (1975) Which elements are excited in electrical stimulation of mammalian central nervous system: a review. *Brain Res* 98:417–440
- Ranck JB (1981) Extracellular stimulation. In: Patterson MM, Kesner RP (eds) *Electrical stimulation research techniques*. Academic Press, New York, pp 1–36

- Rattay F (1987) Ways to approximate current-distance relations for electrically stimulated fibers. *J Theor Biol* 125:339–349
- Reilly JP, Bauer RH (1987) Application of a neuroelectric model to electrocutaneous sensory sensitivity: parameter variation study. *IEEE Trans Biomed Eng BME* 34:752–754
- Reilly JP, Freeman VT, Larkin WD (1985) Sensory effects of transient electrical stimulation – evaluation with a neuroelectric model. *IEEE Trans Biomed Eng BME* 32:1001–1011
- Ritchie JM, Rogart RB (1977) Density of sodium channels in mammalian myelinated nerve fibers and nature of the axonal membrane under the myelin sheath. *Proc Natl Acad Sci USA* 74:211–215
- Ritchie JM, Rogart RB, Strichartz GR (1976) A new method for labelling saxitoxin and its binding to non-myelinated fibres of the rabbit vagus, lobster walking leg, and garfish olfactory nerves. *J Physiol (Lond)* 261:477–494
- Salzman CD, Britten KH, Newsome WT (1990) Cortical microstimulation influences perceptual judgements of motion direction. *Nature* 346:174–177
- Schiller PH, True SD, Conway JL (1979) Paired stimulation of the frontal eye fields and the superior colliculus of the rhesus monkey. *Brain Res* 179:162–164
- Shinoda Y, Arnold AP, Asanuma H (1976) Spinal branching of cortico-spinal axons in the cat. *Exp Brain Res* 26:215–234
- Shizgal P, Conover K, Schindler D (1991) Medial forebrain bundle units in the rat: dependence of refractory period estimates on pulse duration. *Behav Brain Res* 42:151–160
- Singer W, Tretter F, Cynader M (1975) Organization of cat striate cortex: a correlation of receptive field properties with afferent and efferent connections. *J Neurophysiol* 38:1080–1088
- Spruston N, Johnston D (1992) Perforated patch-clamp analysis of the passive membrane properties of three classes of hippocampal neurons. *J Neurophysiol* 67:508–529
- Stoney SD, Thompson WD, Asanuma H (1968) Excitation of pyramidal tract cells by intracortical microstimulation: effective extent of stimulating current. *J Neurophysiol* 31:659–669
- Stuart GJ, Sakmann B (1994) Active propagation of somatic action potentials into neocortical pyramidal cell dendrites. *Nature* 367:69–72
- Stuart G, Spruston N, Sakmann B, Häusser M (1997) Action potential initiation and backpropagation in neurons of the mammalian CNS. *Trends Neurosci* 20:125–131
- Swadlow HA (1974) Properties of antidromically activated callosal neurons and neurons responsive to callosal input in rabbit binocular cortex. *Exp Neurol* 43:424–444
- Swadlow HA (1983) Efferent systems of primary visual cortex: a review of structure and function. *Brain Res Brain Res Rev* 6:1–24
- Swadlow HA (1992) Monitoring the excitability of neocortical efferent neurons to direct activation by extracellular current pulses. *J Neurophysiol* 68:605–619
- Swadlow HA, Weyand TH (1981) Efferent systems of the rabbit visual cortex: laminar distribution of cells of origin, axonal conduction velocities and identification of axonal branches. *J Comp Neurol* 203:799–822
- Szabo I, Milner PM (1972) Self-stimulation in rats: tip alignment influences the effectiveness of bipolar electrodes. *Brain Res* 48:243–250
- Takahashi K (1965) Slow and fast groups of pyramidal tract cells and their respective membrane properties. *J Neurophysiol* 28:908–924
- Tehovnik EJ (1996) Electrical stimulation of neural tissue to evoke behavioral responses. *J Neurosci Methods* 65:1–17
- Tehovnik EJ, Lee K (1993) The dorsomedial frontal cortex of the rhesus monkey: topographic representation of saccades evoked by electrical stimulation. *Exp Brain Res* 96:430–442
- Thomson AM, West DC (1993) Fluctuation in pyramid-pyramid excitatory synaptic potentials modified by presynaptic firing pattern and postsynaptic membrane potential using paired intracellular recording in rat neocortex. *Neuroscience* 54:329–346
- Thomson AM, Gilderstone D, West DC (1988) Voltage-dependent currents prolong single-axon postsynaptic potentials in layer III pyramidal neurons in rat neocortical slices. *J Neurophysiol* 60:1896–1907
- Thomson AM, Deuchars J, West DC (1993) Large, deep layer pyramid-pyramid single axon EPSPs in slices of rat motor cortex display paired pulse and frequency-dependent depression, mediated presynaptically and self facilitation, mediated postsynaptically. *J Neurophysiol* 70:2354–2369
- Tkacs NC, Wurster RD (1991) Strength-duration and activity-dependent excitability properties of frog afferent axons and their intraspinal projections. *J Neurophysiol* 65:468–476
- Volgushev M, Voronin LL, Chistiakova M, Artola A, Singer W (1995) All-or-none excitatory postsynaptic potentials in the rat visual cortex. *Eur J Neurosci* 7:1751–1760
- Weiss G (1901) Sur la possibilité de rendre comparables centre eux les appareils servant à l'excitation électrique. *Arch Ital Biol* 35:413–446
- West DC, Wolstencroft JH (1983) Strength-duration characteristics of myelinated and non-myelinated axons in the cat spinal cord. *J Physiol (Lond)* 337:37–50
- Westenbroek RE, Merrick DK, Catterall WA (1989) Differential subcellular localization of RI and RII Na⁺ channel subtypes in central neurons. *Neuron* 3:695–704
- Yeomans JS, Tehovnik EJ (1988) Turning responses evoked by stimulation of visuomotor pathways. *Brain Res Brain Res Rev* 13:235–259